Susceptibility of Alloy 22 to Environmentally Assisted Cracking in Yucca Mountain Relevant Environments

J.C. Estill, K.J. King, D.V. Fix, D.G. Spurlock, G.A. Hust,
S.R. Gordon, R.D. McCright, R.B. Rebak, G.M. Gordon

U.S. Department of Energy

Lawrence
Livermore
National
Laboratory

January 30, 2002

SUSCEPTIBILITY OF ALLOY 22 TO ENVIRONMENTALLY ASSISTED CRACKING

IN YUCCA MOUNTAIN RELEVANT ENVIRONMENTS

John C. Estill, Kenneth J. King, David V. Fix, Darryl G. Spurlock, Gary A. Hust, Steven R. Gordon, R. Daniel McCright and Raúl B. Rebak

Lawrence Livermore National Laboratory, Livermore, CA, 94550

Gerald M. Gordon

Framatome – Bechtel SAIC, Las Vegas, NV, 89134

ABSTRACT

In its current design, the high level nuclear waste containers will include an external layer of Alloy 22 (Ni-22Cr-13Mo-3W-3Fe). Since over their life-time the containers may be exposed to multi-ionic aqueous environments, a potential degradation mode of the outer layer could be environmental assisted cracking (EAC). The objective of the current research work was to quantify the susceptibility of Alloy 22 to EAC in a several environmental conditions including solution composition, temperature and electrochemical potential. The susceptibility to EAC was evaluated using the constant deformation technique, the compact specimen - low cycle fatigue method and the slow strain rate test (SSRT). The alloy was tested in the wrought mill annealed (MA) and in the as-welded conditions. Results show that Alloy 22 was extremely resistant to EAC in a wide range of environmental conditions. Using SSRT, Alloy 22 was found susceptible to EAC in one electrolyte at one temperature and at one electrochemical potential.

Keywords: high level nuclear waste, nickel-based alloy, N06022, environmentally assisted cracking, U-bend, slow strain rate test, compact specimens, crack propagation rate, simulated acidified water (SAW), simulated concentrated water (SCW), basic saturated water (BSW), simulated saturated water (SSW).

INTRODUCTION

The current design concept for the high level nuclear waste containers in the USA is based on a metallic multi-barrier system. This design specifies a 2-cm thick external layer of Alloy 22 (UNS N06022) and a 5-cm thick internal layer of type 316 stainless steel (UNS S31603).[1] The main purpose of the internal barrier is to provide structural integrity and to contribute to the shielding of radiation. The main role of the external barrier is to provide protection against corrosion. Alloy 22 was selected for the external barrier due to its excellent resistance to general corrosion, localized corrosion and environmentally assisted cracking in a broad range of environments.[1-9] Alloy 22 is a nickel (Ni) based alloy that contains approximately 22% chromium (Cr), 13% molybdenum (Mo), 3% tungsten (W) and 3% iron (Fe). By virtue of its high level of Cr, Alloy 22 remains passive in most industrial environments and therefore has an exceptionally low general corrosion rate. The combined presence of Cr, Mo and W imparts Alloy 22 with high resistance to localized corrosion such as pitting corrosion and crevice corrosion. Mill annealed Alloy 22 is also highly resistant to EAC in acidic concentrated chloride solutions.[6-7] However, alloy 22 may be susceptible to EAC under other severe environmental conditions.[7,10] For example, Andresen et al. tested the susceptibility of Alloy 22 at its corrosion potential (E_{corr}) to EAC in air saturated concentrated multi-ionic solutions at 110°C. Multi-ionic solutions are the most likely environment that may be encountered at the permanent repository site in Yucca Mountain.[11] Using the reverse DC potential technique, Andresen et al. reported a crack grow rate of 5 x 10^{-13} m/s in a 20% cold worked specimen loaded to a stress intensity of 30 MPa.m$^{1/2}$. The measured crack growth rate was near the detection limit of the system.[10]

The purpose of the present work was to use several testing techniques to study further the susceptibility of Alloy 22 to EAC in a variety of environments that could be related to the permanent emplacement site. These environments are expected to be multi-component in nature.[11]

EXPERIMENTAL TECHNIQUE

The specimens used to assess susceptibility of Alloy 22 to EAC were machined from sheet or plate stock. The typical mechanical properties of MA plate and sheet material are listed in Table 1. The surface finish of the specimens was in the as-machined condition, which corresponded to an average roughness of approximately 32. All the specimens were degreased in acetone before testing. Table 2 shows four typical chemical compositions of some of the heats of materials used for this study. For certain type of tests (e.g. single U-bend) more than one heat chemistry may have been used. Susceptibility of Alloy 22 to EAC was evaluated using the following testing methods: (a) Constant Deformation Tests (Single and Double U-bend samples), (b) Reversed DC potential tests (Compact Tension samples) and (c) Slow Strain Rate Tests (SSRT). Details about specimen shape and testing procedures are given in each one of the results sections.

A few of the electrolyte solutions for EAC testing were simple salt solutions but most were complex solutions containing several ionic species. Table 3 shows the composition of the multi-component electrolyte solutions mentioned in this paper. Most of the tests were carried out at ~ 22°C (ambient), 60°, 90°C, 95°C, 105°C and 120°C. The electrolyte solutions were naturally aerated, that is, the solutions were not purged and the ingress of air above the solution level was not restricted. All tests were carried under ambient pressure. The electrochemical potentials in this paper are reported in the silver-silver chloride scale [SSC]. At ambient temperature, the SSC scale is 222 mV more positive than the normal hydrogen electrode (NHE). After testing, the samples were evaluated using optical and scanning electron microscopy.

EXPERIMENTAL RESULTS AND DISCUSSION

Constant Deformation Tests (U-bend Specimens)

Two types of U-bend specimens were used. Most of the constant deformation tests were carried out using single U-bend specimens; however, a few tests were done using double U-bend specimens. Single U-bend specimens were produced by bending a 0.062-inch (~1.6 mm) thick, 0.75 inch (19 mm) wide and 2.5-inch (64 mm) long strip of Alloy 22 over a metallic die. The resulting specimen had a constant separation between both legs or ends of 0.5 inch (~13 mm) secured by a bolt, which was electrically insulated from the specimen through ceramic washers. Thus, each single U-bend sample had two metal-ceramic artificially formed crevices. The total plastic deformation in external outer fiber of Alloy 22 was approximately 12%. Single U-bends were produced using both wrought sheets and welded sheets (Table 1). In the welded (W) specimens, the weld was along the apex of the bend. The weld process was gas metal arc welding (GMAW) using filler metal and the seam had full penetration. The specimens were exposed to large tanks containing approximately 1000-liter electrolyte solutions SAW, SDW and SCW at 60°C and 90°C for up to 4 years. Some specimens were fully immersed in the electrolyte solution (L) and some specimens were exposed above the water line or vapor phase (V). Table 4 summarizes the array of specimens that were examined. Examination was carried out using a 40 times magnification in a stereomicroscope. Most of the specimens were completely featureless, that is, they appeared shiny metallic as the non-tested condition. Only a few specimens appeared to have changed in color. For example, the specimens exposed to 4 years in SAW at 90°C had a shiny brown-golden color. A related but almost unperceivable color was detected in the specimens exposed for 24 months in SAW at 60°C. The origin of the color is not fully understood yet, but it is probable a combination of salts and rust that may have deposited from the electrolyte. Nonetheless, none of the 145 specimens examined, either wrought or welded, had evidences of environmentally assisted cracking (Table 4).

The double U-bend specimens were produced by bending two strips of metal simultaneously, thus producing a tight crevice between the strips. Each strip was 0.75-inch (19 mm) wide, 0.062-inch (1.6 mm) thick and approximately 5-inch (127 mm) long before deformation. The ends or legs of each specimen were secured to a fixed distance with an insulated bolt. The plastic deformation at the outer fiber was approximately 5-7%. Two double U-bend specimens were tested at the corrosion potential for 17 months in naturally aerated BSW solution (Table 3) at 105°C. Examinations after test showed that the specimens were free of cracking either from the bulk side of the solution or from the creviced area. Moreover, the specimens were completely featureless, that is, they did not change in color or suffered any type of corrosion either from the bulk or from the metal/metal creviced side.

Results from the constant deformation tests confirm that alloy 22 was extremely resistant to EAC in the mill annealed or as-welded condition when exposed to multi-ionic aqueous environments at the corrosion potential. The corrosion potential was not the same for all tests reported above and in Table 4. For example, preliminary results show that the corrosion potential could vary from –0.1 V for specimens immersed in BSW at 105°C for six months to +0.3 V for specimens immersed in SAW at 90°C for 4 years. It is likely that the higher corrosion potential in SAW solution was a result of rust contained in the electrolyte or deposited on the specimen surface. The most typical values of corrosion potential are in the vicinity of 0 V. Considering a detection limit with the stereomicroscope of 100 μm (between 5 and 10% of the specimen thickness), a four-year immersion of U-bend specimens could have detected an average

3

crack propagation rate of 8 x 10^{-13} m/s (with induction time = 0). That is, if Alloy 22 was susceptible to EAC under constant deformation conditions, average crack propagation rate should be below 10^{-13} m/s.

Reverse DC Method (Compact Specimens for crack propagation)

Crack growth rate (CGR) was monitored using compact tension specimens (CT) and the reverse DC potential drop technique. The detection limit for crack growth of this technique is in the order of 1 μm.[10] Tests were conducted using specimens made from wrought MA alloy. These compact specimens were 1-inch (25.4 mm) wide, 2.5-inch (63.4 mm) long and 2.4-inch (61 mm) tall. They had a 1.35-inch (34 mm) long notch and 0.05-inch (1.3 mm) deep grooves following the notch on each side of the specimen. The CT specimens also had a fatigue crack produced in air prior to testing in the electrolyte. The fatigue crack was produced at a maximum stress intensity of 30 MPa.m$^{1/2}$, a frequency of 0.01 Hz and a stress ratio R = 0.7. To minimize the cold worked area in front of the fatigue crack, the stress intensity was gradually reduced as the fatigue crack progressed. The fatigue crack length was typically 2.5-mm. In general, in this technique, the tests are carried out by promoting the formation of an environmentally assisted crack in the electrolyte and temperature of interest by using a cyclic loading at a frequency of 0.01 to 0.001 Hz while monitoring the crack length. Subsequently, crack propagation is monitored during periods at which a constant load is applied to the specimen. If crack propagation arrests, crack growth may be revived by another sequence of cyclic loading. Tests reported in this paper were carried out by triplicate in naturally aerated SAW and SCW electrolytes (Table 3) at 95°C. The tests were carried out at the corresponding corrosion potential. The maximum applied stress intensity during the tests was 45 MPa.m$^{1/2}$ and the total testing time was approximately 10 months. Table 5 shows the results of maximum crack growth at the two main stages of testing. During load cycling, crack growth rate appears to be two orders of magnitude higher than the crack growth rate in periods where a constant load was applied to the specimens. The results reported in Table 5 are in the same order of magnitude that those reported by Andresen et al. even though the testing conditions were not identical.[10] Andresen et al. have stated that a 20% cold worked Alloy 22 specimen may be cracked at a rate of 5 x 10^{-13} m/s in BSW solution at 105°C under a constant load of 30 MPa.m$^{1/2}$.[10] Table 5 also shows that solution SCW appears to be more aggressive towards EAC than SAW solution. Table 3 shows that pH of solution SCW is alkaline and contains fluoride ions while solution SAW contains chloride ions and is acidic. Moreover, solution SAW contains four times as much nitrate than SCW. Ni-Cr-Mo alloys such as Alloy 22 are resistant to EAC in acidic chloride solutions;[6,7] however they may be susceptible to EAC in solutions containing fluoride ions.[7] Moreover, it is likely that nitrate would act as an inhibitor to EAC in SAW by increasing the repassivation rate of a damaged passive film in Alloy 22.

Slow Strain Rate Tests (SSRT)

Specimens were prepared from wrought mill annealed Alloy 22 plate (Table 2). Each specimen was cylindrical, approximately 7.25-inch (184 mm) long and 0.438-inch (11 mm) diameter. The useful gage of the specimens was 1-inch (25.4 mm) long and had a 0.1-inch (2.54 mm) diameter. Only the useful gage section was exposed to the electrolyte solution. Non-important areas of the specimens were covered with a protective coating. The slow strain rate tests were conducted at a constant deformation rate of 1.6 x 10^{-6} s^{-1}. Table 6 shows the experimental results. One specimen was strained to rupture in air as a reference test for an inert-like environment. Table 6 shows the maximum stress during straining, the time to failure and the reduction in area of the specimens at the time of failure. The susceptibility to stress corrosion cracking in the aqueous environments can be assessed by comparing these three parameters above with the same parameters in air. Straining of the specimens to rupture was performed both at the corrosion potential and at constant applied potentials. Table 6 shows that out of 18 SSRT performed, only two

4

samples (112 and 021) showed evidence of EAC. Experiments carried out in SAW at the corrosion potential (Samples 015-017 and 003) showed that the presence of soluble lead did not increase the susceptibility of Alloy 22 to EAC. Experiments carried out in BSW solution at +0.4 V (Samples 119, 120, 115 and 129 in Table 6) show that the removal of nitrate or sulfate from the solution did not increase the susceptibility of Alloy 22 to EAC.

Figure 1 shows the ratio of the maximum stress and the time to failure for specimens strained in four aqueous solutions at the corrosion potential (Samples 012, 004, 013, 015 and 127 in Table 6). Figure 1 shows that all the specimens had a maximum stress and time to failure environment/air ratios of 0.95 or higher, indicating little susceptibility of Alloy 22 to EAC at the corrosion potential (-0.2 to +0.3 V) (Table 6). Figure 2 shows stress/elongation curves for specimens strained at an applied potential of 0.4 V in three different solutions (Samples 012, 119, 125 and 021 in Table 6). Even though the testing temperature in Figure 2 was not constant, data show that the elongation to failure in environments SSW and BSW was similar to the elongation to failure in air, indicating little decrease of ductility of Alloy 22 in these two environments. However, the elongation to failure in SCW solution was approximately 25% shorter than the elongation to rupture in air, indicating that alloy 22 might be susceptible to EAC in SCW at the anodic potential of +0.4 V. Figures 3-5 show the fracture end of the specimens strained in air (012), in BSW (119) at +0.4 V and in SCW at +0.4 V (112), respectively. It is apparent that the specimen strained in SCW (Figure 5) had less reduction in area than the specimens shown in Figures 3-4. Moreover, Figure 5 shows that the specimen had secondary EAC cracking, which was of transgranular (TG) mode (Figure 6). Figure 7 shows that this TG cracking was shallow. Considering a zero induction time, crack propagation for Sample 112 was in the order of 10^{-10} m/s. When Alloy 22 was strained at +0.4 V but at 22°C (Sample 020 in Table 6), it did not suffer EAC cracking. Currently, the windows of temperature and electrochemical potential for susceptibility of Alloy 22 to EAC are being explored further.

The SSRT technique is highly aggressive since it forces the specimen to deform under the chosen environmental conditions until rupture is achieved. Nevertheless, in most of the tested environments, the time to failure and the fracture mode of these specimens were undistinguishable from those of the specimen tested in air. The only condition that produced a case of EAC in Alloy 22 was SCW solution at 73°C and at an applied potential of +0.4 V. Crack propagation studies described before seem to suggest that the SCW solution would be more aggressive than SAW solution or BSW solution. At this moment it can be speculated that the presence of fluoride and the low presence of oxyanions in SCW (Table 3) might have contributed to this enhanced aggressiveness. However, this subject needs to be explored further in future studies.

CONCLUSIONS

(1)   Mill annealed (MA) and welded Alloy 22 is highly resistant to environmentally assisted cracking (EAC) in multi-ionic solutions that could be found in Yucca Mountain.

(2)   U-bend samples exposed for up to 4 years in SAW, SCW and SDW solutions at 60°C and 90°C were free from EAC.

(3)   Using a combination of low cycle fatigue and constant load testing, crack growth rates in the order of 10^{-13} m/s can be induced in MA Alloy 22 in SAW and SCW at 95°C and at a stress intensity of 45 MPa.m$^{1/2}$.

(4)   Slow strain rate tests (SSRT) showed that MA Alloy 22 is extremely resistant to EAC in a variety of environments both at the corrosion potential and at anodic potentials. EAC was only found in SCW at 73°C and at an applied potential of +0.4 V.

(5)   SCW appears to be the most aggressive of the tested environments to Alloy 22 EAC.

ACKNOWLEDGMENTS

REFERENCES

1. D. S. Dunn, G. A. Cragnolino and N. Sridhar in Scientific Basis for Nuclear Waste Management XXIII, Materials Research Society, (Warrendale, PA 2000), pp. 89-94.
2. P. E. Manning, J. D. Schöbel, Werkstoffe und Korrosion, 37, 137-145 (1986).
3. S. J. Lukezich, The Corrosion Behavior of Ni-Base High Performance Alloys in Simulated Repository Environments, MS Thesis, The Ohio State University, 1989.
4. K. A. Gruss, G. A. Cragnolino, D. S. Dunn, N. Sridhar, Paper 149, Corrosion/98, NACE International, (Houston, TX 1998).
5. R. B. Rebak and P. Crook, in Critical Factors in Localized Corrosion III, The Electrochemical Society, Volume 98-17, (Pennington, NJ 1999), pp. 289-302.
6. Y-M. Pan, D. S. Dunn and G. A. Cragnolino in Environmentally Assisted Cracking: Predictive Methods for Risk Assessment and Evaluation of Materials, Equipment and Structures, ASTM STP 1401, (West Conshohocken, PA 2000), pp. 273-288.
7. R. B. Rebak in Environmentally Assisted Cracking: Predictive Methods for Risk Assessment and Evaluation of Materials, Equipment and Structures, ASTM STP 1401, (West Conshohocken, PA 2000), pp. 289-300.
8. R. B. Rebak in Corrosion and Environmental Degradation, Volume II, Wiley-VCH (Weinheim, Germany 2000), pp. 69-111.
9. D. S. Dunn and C. S. Brosia, Paper 125, Corrosion/01, NACE International, (Houston, TX 2001).

10. P. L. Andresen, P. W. Emigh, L. M. Young and G. M. Gordon, Paper 130, Corrosion/01, NACE International, (Houston, TX 2001).
11. N. D. Rosenberg, G. E. Gdowski and K. G. Knauss, Applied Geochemistry, 16 (2001), pp. 1231-1240.

TABLE 1
TYPICAL MECHANICAL PROPERTIES OF PLATE AND SHEET ALLOY 22

Heat	Tensile Strength [UTS] (MPa)	Yield Stress [0.2%] (MPa)	Elongation to Rupture (%)	Hardness (RB)	ASTM Grain Size
Sheet – 2277-8-3203	824	412	62	92	5.5
Plate – 2277-8-3126	766	387	64.4	83	4

TABLE 2
CHEMICAL COMPOSITION OF THE STUDIED ALLOY 22 HEATS (Wt%)

Element	Single U-bend (Heat 2277-0-3264)	Double U-bend (Heat 2277-8-3203)	Compact (Heat 2277-8-3163)	SSRT (Heat 2277-6-3126)
C	0.004	0.002	0.003	0.004
Co	1.14	1.82	0.87	1.03
Cr	21.3	21.30	21.61	21.70
Fe	4.4	4.00	4.17	3.59
Mn	0.29	0.19	0.25	0.27
Mo	13.4	13.08	13.46	13.26
Ni	~56	~57	~57	~57
P	0.01	<0.005	0.009	0.006
S	<0.002	0.008	0.002	0.001
V	0.17	0.14	0.16	0.14
W	2.9	2.93	2.81	2.80

TABLE 3
CHEMICAL COMPOSITION OF THE ELECTROLYTE SOLUTIONS (mg/L)

Ion	SDW pH 10.1	SCW pH 10.3	SAW pH 2.8	SSW pH 6.7	BSW pH 13
K^+	34	3400	3400	141,600	81,480
Na^+	409	40,900	40,900	487,000	231,225
Mg^{2+}	1	< 1	1000	---	---
Ca^{2+}	0.5	< 1	1000	---	---
F^-	14	1400	0	---	1616
Cl^-	67	6700	24,250	128,000	169,204
NO_3^-	64	6400	23,000	1,313,000	177,168
SO_4^{2-}	167	16,700	38,600	---	16,907
HCO_3^-	947	70,000	0	---	107,171
SiO_3^{2-}	~ 40	~ 40	~ 40	---	9038

TABLE 4
CONSTANT DEF0RMATION (U-BEND) TESTS OF ALLOY 22.
NUMBER OF EXAMINED SPECIMENS: W = WELDED, L = LIQUID, V = VAPOR.

Testing Time (months)	SAW, 60°C	SAW, 90°C	SCW, 60°C	SCW, 90°C	SDW, 60°C	SDW, 90°C
6	3L, 3v, 3WL, 3wv	3L, 3v	3L, 3v, 3WL, 3wv	3L, 3v, 3WL, 3wv	1L, 1v, 1WL, 1wv	1L, 1v, 2WL, 2wv
12	3L, 3v, 3WL, 3wv	3L, 3v	3L, 3v, 1WL, 3wv	3L, 3v, 3WL, 3wv	1L, 1v, 1WL, 1wv	1L, 1v, 2WL, 2wv
24	3L, 3L					
27						1L, 1v, 1WL, 1wv
28				3L, 3v, 1WL, 1wv	1L, 1v, 1WL, 1wv	
29		3L, 3v, 1WL, 1wv	3L, 3v, 1WL, 1wv			
48		2L				
Total Specimens	30	22	30	35	12	16

8

TABLE 5
COMPACT TENSION / REVERSE DC TESTING OF ALLOY 22
MAXIMUM APPLIED STRESS INTENSITY = 45 MPa.m$^{1/2}$

Conditions	Approximate Maximum CGR at R = 0.7 and 0.001 Hz	Approximate Maximum CGR at Constant Load
SAW – 95°C	2-3 x 10^{-11} m/s	2 x 10^{-13} m/s
SCW – 95°C	3 x 10^{-11} m/s	5 x 10^{-13} m/s

TABLE 6
SLOW STRAIN RATE TESTING OF MA ALLOY 22
STRAIN RATE: ~ 1.6 x 10^{-6} s^{-1}.

Sample	Environment	T (°C)	E_{corr}	E Applied	Time to Failure (h)	Max. Stress (MPa)	RA (%)	Observations
012	Air	22	N/A	N/A	124	786	74	Inert
123	4 M NaCl pH ~ 6	98	-323	+350	127	758	80	No EAC
004	Saturated CaCl$_2$ (~17 molal), pH ~ 6	120	-140 to -180	E_{corr}	127	752	71	No EAC
013	1% PbCl$_2$, pH ~4	95	---	E_{corr}	126	765	72	No EAC
015	SAW, pH ~ 3	63	-7 to +360	E_{corr}	118	758	79	No EAC
016	SAW + 0.005% Pb(NO$_3$)$_2$, pH ~ 3	76	-6 to +370	E_{corr}	124	772	74	No EAC
017	SAW + 0.005% Pb(NO$_3$)$_2$, pH ~ 3	76	0 to +350	E_{corr}	125	772	74	No EAC
003	SAW + 0.005% Pb(NO$_3$)$_2$, pH ~ 3	95	-90 to +400	E_{corr}	118	752	85	No EAC
127	BSW – [NO$_3^-$ + SO$_4^=$], pH ~ 13 [1]	98	-240 to -220	E_{corr}	123	745	72	No EAC
124	BSW – [NO$_3^-$ + SO$_4^=$], pH ~ 13	105	-330	+100	120	745	78	No EAC
122	BSW – [NO$_3^-$ + SO$_4^=$], pH ~ 13	98	-245	+200	122	752	72	No EAC
119	BSW, pH ~ 13	105	-301	+400	118	745	75	No EAC
120	BSW, pH ~ 13	105	-323	+400	99	745	74	No EAC
115	BSW – NO$_3^-$, pH ~ 13	105	-335	+400	115	752	77	No EAC
129	BSW – SO$_4^=$, pH ~ 13	105	-314	+400	119	731	82	No EAC
125	SSW, pH ~ 6	100	-154	+400	113	717	71	No EAC
112	SCW, pH ~ 9	73	-94	+400	91	696	71	EAC
020	SCW, pH ~ 9	22	-109	+400	116	800	85	No EAC
021	SCW, pH ~ 9	73	-171	+400	90	662	64	EAC

RA: Reduction in area at time of rupture. [1] BSW without the presence of nitrate or sulfate.
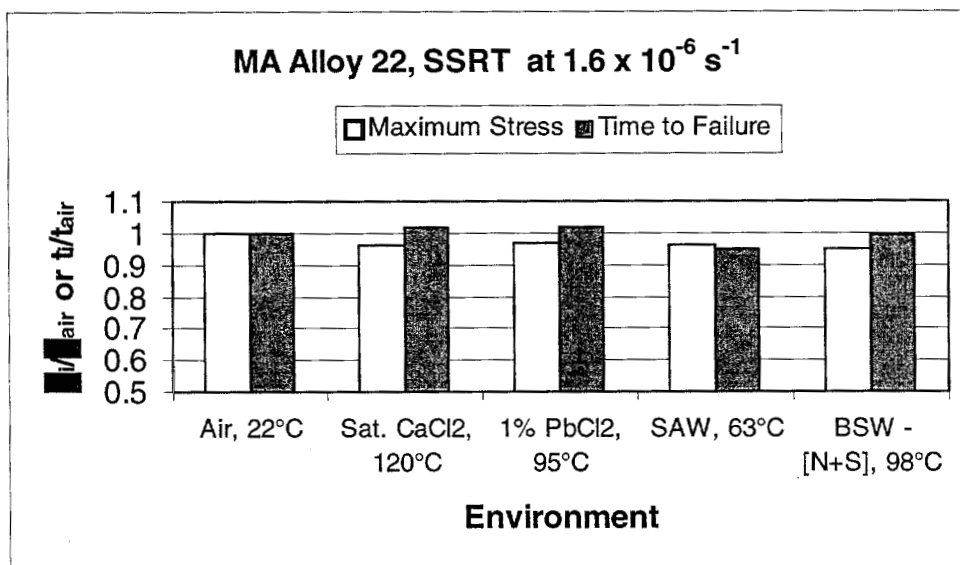
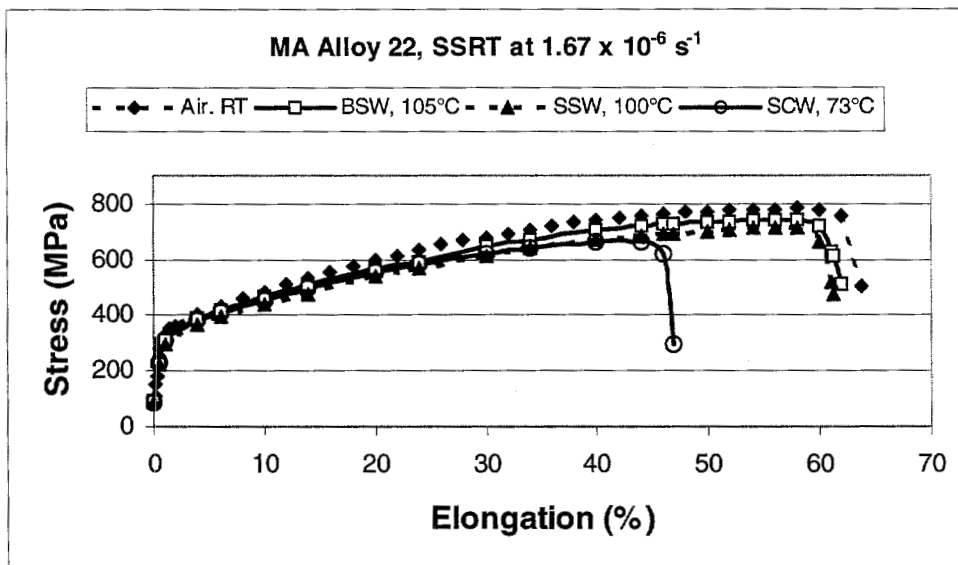FIGURE 1: Stress and time ratios for specimens strained at E_{corr}.

FIGURE 2: Stress-Elongation curves for specimens strained at +0.4 V.
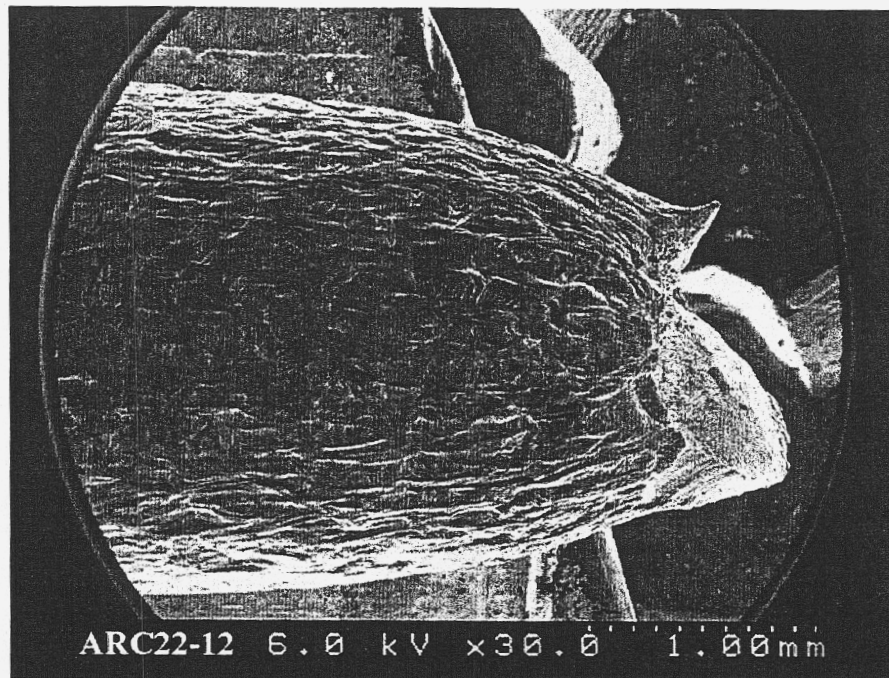
10

FIGURE 3: Fracture end of specimen strained in air at ambient temperature.
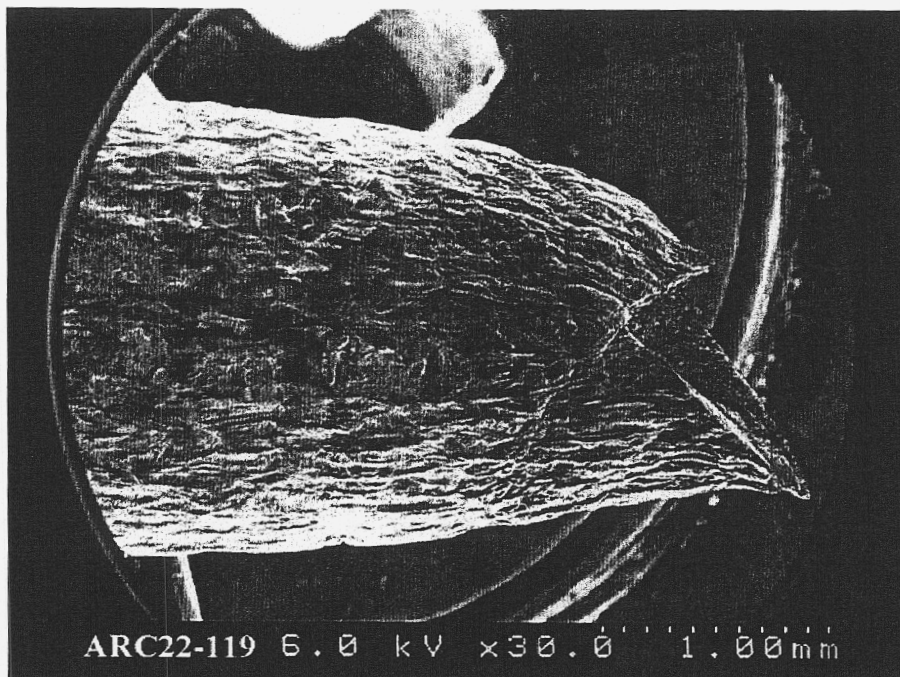Magnification X 30.

FIGURE 4: Fracture end of specimen strained in BSW at 105°C and +0.4 V.
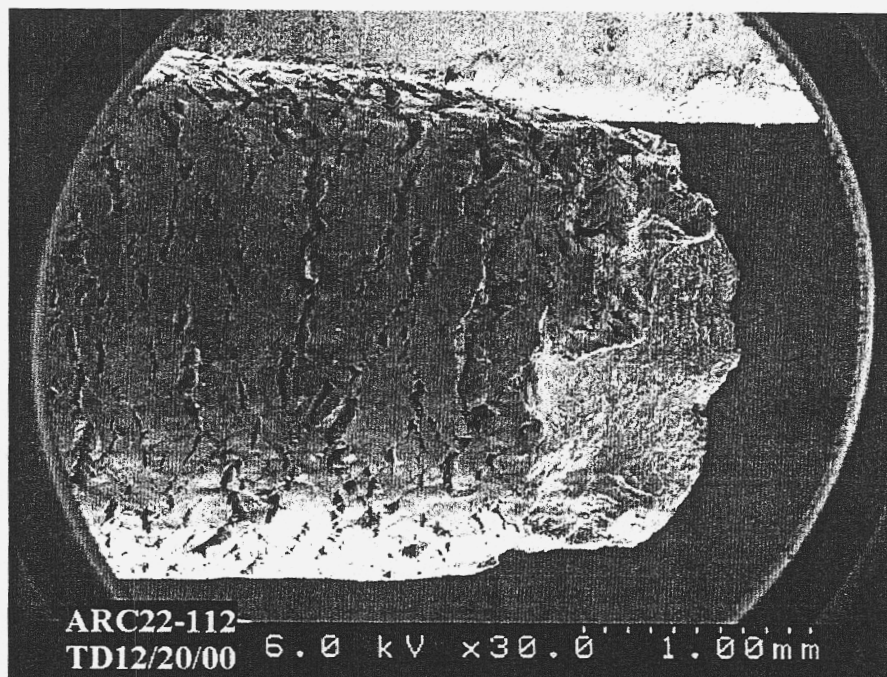Magnification X 30.

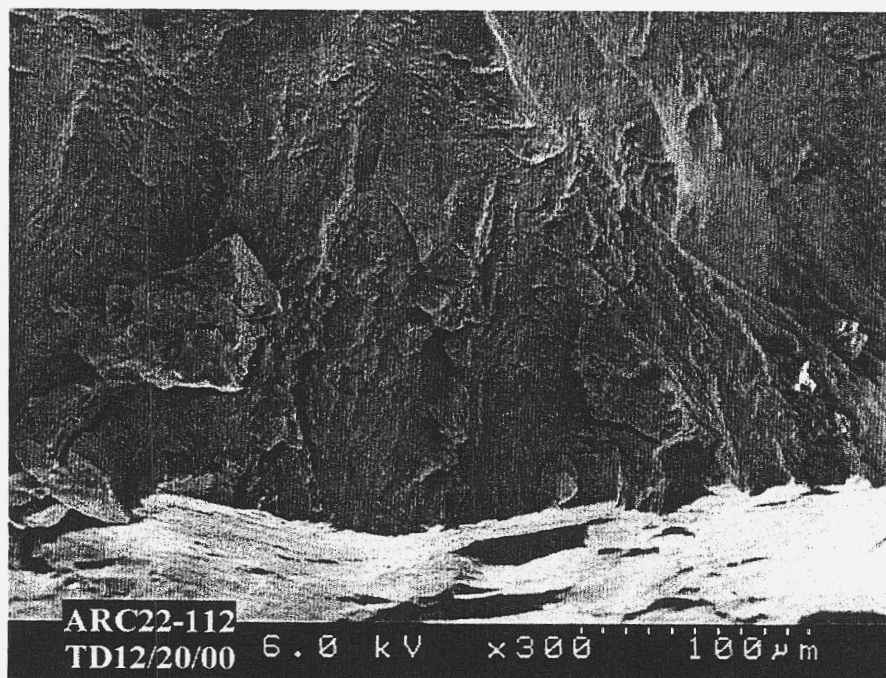FIGURE 5: Fracture end of specimen strained in SCW at 73°C and +0.4 V. Magnification X 30.

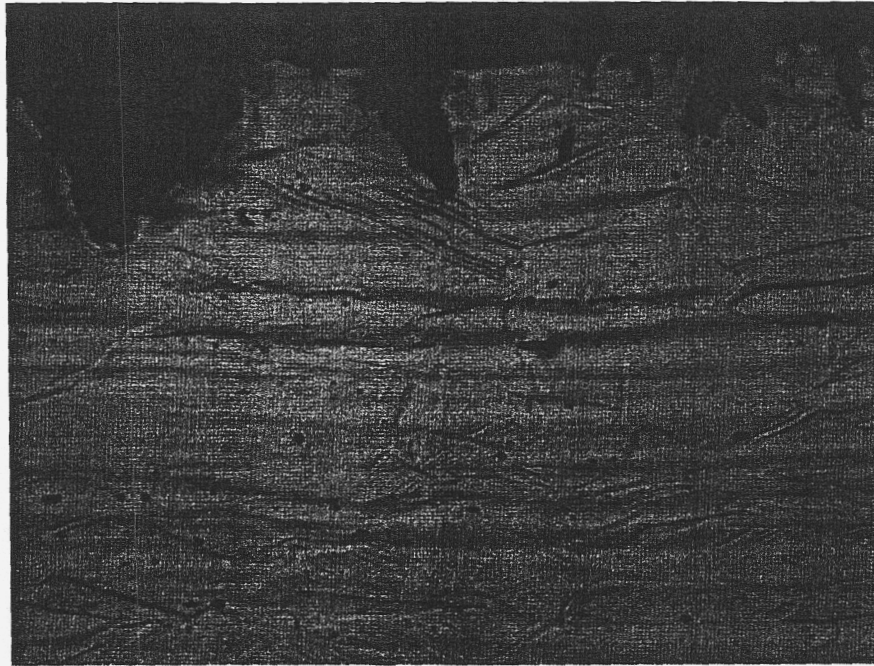FIGURE 6: Fracture surface of specimen strained in SCW at 73°C and +0.4 V. Magnification X 300.

FIGURE 7: Metallographic sectioning of specimen strained in SCW at 73°C and +0.4 V (Sample 112). Magnification X 200.